Recent advances in Rail Vehicle Moving Source Beamforming

Bernard Ginn[1], Jesper Gomes[2], and Jørgen Hald[3]

[1,2,3] Brüel & Kjær Sound & Vibration Measurement A/S,

Skodsborgvej 307, 2850 Nærum, Denmark

ABSTRACT

A measurement technique is described for the localization and visualization of noise sources on moving rail vehicles using beamforming. The Delay-And-Sum (DAS) beamforming, is often used on stationary (fixed) sources. However the method can also be applied to moving sources such as rail vehicles, road vehicles and aircraft fly-overs, as well as rotating blades on wind turbines. Recently, deconvolution techniques have been introduced as post-processing after DAS to improve the spatial resolution and reduce the level of ghost sources in the calculated noise maps. This paper describes a commercially available system which includes DAS and deconvolution techniques, dedicated to the rail vehicle industry. Special consideration is paid to the configuration of the test site and its influence on the measurement results. The advantages of various microphone array designs for measurements on bogies, rails and pantographs are discussed. Guidelines are given for the selection of an appropriate array (half-wheel, logarithmic wheel) for the source of interest and illustrated with practical results from noise emission measurements on regional trains.
Keywords: Beamforming, Array, railways

1. INTRODUCTION

Beamforming is an array-based measurement technique for sound source localisation from medium to long measurement distances. Basically, the source localisation is performed by estimating the amplitudes of plane (or spherical) waves incident towards the array from a chosen set of directions. The angular resolution is inversely proportional to the array diameter measured in units of wavelength, so the array should be much larger than the wavelength to get a fine angular resolution. At low frequencies, this requirement usually cannot be met, so here the resolution will be poor. For typical, irregular array designs, the beamforming method does not allow the measurement distance to be much smaller than the array diameter. On the other hand, the measurement distance should be kept as small as possible to achieve the finest possible resolution on the source surface. This is of course not possible when measuring on large objects, because the calculation area is limited by the angular coverage. The use of a discrete set of measurement points on a plane can be seen as a spatial sampling of the sound field. Nearfield Acoustical Holography, NAH as well as SONAH (Statistically Optimized NAH) require a grid spacing less than half a wavelength at the highest frequency of interest [3]. At higher frequencies the number of required measurement points becomes very high. When the grid spacing exceeds half a wavelength, spatial aliasing components or interpolation errors quickly get very disturbing. Compared to the performance of a regular grid of microphones, the use of optimized, irregular arrays can reduce the spatial aliasing effects to an acceptable level up to a much higher

[1] KevinBernard.Ginn@bksv.com
[2] Jesper.Gomes@ bksv.com
[3] Jorgen.Hald@ bksv.com

frequency with the same average spatial sampling density. This indicates why beamforming can measure up to high frequencies and provide a good resolution with a fairly low number of microphones. Thus beamforming is an attractive alternative and supplement to NAH/SONAH, because measurements can be taken at some intermediate distance from the source with a highly sparse array. Furthermore at high frequencies, beamforming can provide quite good resolution.

2. THEORY OF BEAMFORMING

As illustrated in Fig. 1, we consider a planar array of M microphones at M distributed locations r_m (m=1,2,….,M) in the xy-plane of the coordinate system. When such an array is applied for Delay-And-Sum (DAS) beamforming, the measured pressure signals p_m are individually delayed and then summed [1],[2]:

$$b(\boldsymbol{\kappa},t)=\sum_{m=1}^{M} p_m(t-\Delta_m(\boldsymbol{\kappa})) \tag{1}$$

The individual time delays Δ_m are chosen with the aim of achieving selective directional sensitivity in a specific direction, characterized here by a unit vector $\boldsymbol{\kappa}$. This objective is met by adjusting the time delays in such a way that signals associated with a plane wave, incident from the direction κ, will be aligned in time before they are summed. Geometrical considerations (see Fig. 1) show that this can be obtained by choosing:

$$\Delta_m=\frac{\boldsymbol{\kappa}\cdot\mathbf{r}_m}{c} \tag{2}$$

where c is the propagation speed of sound. Signals arriving from other far-field directions will not be aligned before the summation, and therefore they will not coherently add up.

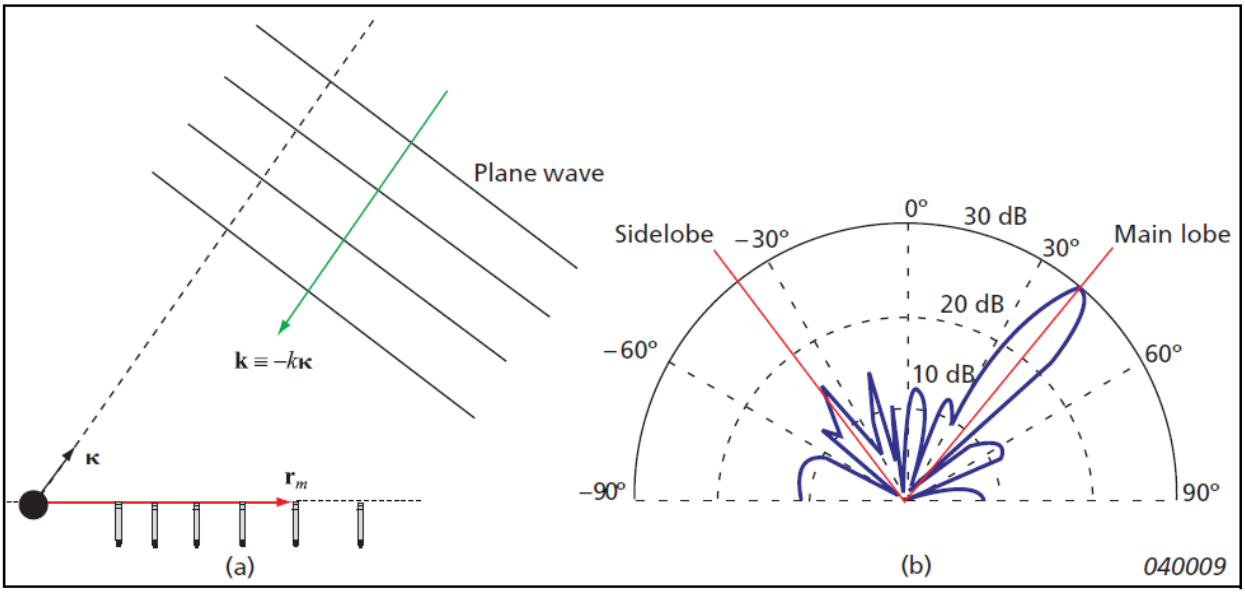

Figure 1 – (a) A microphone array, a far-field focus direction, and a plane wave incident from the focus direction. (b) Directional sensitivity diagram with a main lobe in the focus direction and lower side lobes in other directions

The frequency domain version of Eq. (1) for the Delay-And-Sum beamformer output is:

$$B(\boldsymbol{\kappa},\omega)=\sum_{m=1}^{M} P_m(\omega)\cdot e^{-j\omega\Delta_m(\boldsymbol{\kappa})}=\sum_{m=1}^{M} P_m(\omega)\cdot e^{j\mathbf{k}\cdot\mathbf{r}_m} \tag{3}$$

Here, ω is the temporal angular frequency, $\mathbf{k} \equiv -k\boldsymbol{\kappa}$ is the wave number vector of a plane wave incident from the direction $\boldsymbol{\kappa}$ in which the array is focused (see Fig. 1) and $k=\omega/c$ is the wave number. In Eq. (3) an implicit time factor equal to $e^{j\omega t}$ is assumed.

The frequency domain beamformer has a main lobe of high directional sensitivity around the focus direction and lower sensitivity in other directions, with lower side lobes. The relative difference in dB between the main lobe and the highest side lobe is known as the Maximum Side Lobe (MSL) suppression and is widely used as a quality indicator of acoustic arrays. The main lobe width is inversely proportional to the diameter D of the array. It can be shown that the main lobe width defines an on-axis angular resolution equal to λ/D, where λ is wavelength. At a measurement distance equal to L this angular resolution corresponds to a spatial resolution, R, given by the expression

$$R = \frac{L}{D}\lambda \tag{4}$$

The measurement distance L should not be much smaller than the array diameter D otherwise too much emphasis will be placed on the measurements from microphones near the centre of the arrray . For comparison, NAH provides a resolution around $\lambda/2$ at high frequencies and approximately equal to the measurement distance L at lower frequencies. Thus, at low frequencies NAH can provide significantly better resolution, when a sufficiently small measurement distance is used.

3. BEAMFORMING WITH INCREASED SPATIAL RESOLUTION

Using iterative deconvolution techniques it is possible to achieve a higher resolution than that provided by standard DAS beamforming techniques [4] The idea is that when measuring on a point source, the DAS beamforming pressure power result is given by the location of the point source convolved by the beamformer's directional characteristics as shown in Fig. 1(b) and produces what is known as the point-spread function, PSF. For a given beamformer array design, this PSF is known and can be compensated for using deconvolution techniques. This deconvolution gives a possibility to increase the spatial resolution of acoustic arrays and reduce disturbing side lobe effects. In many fields of imaging, for example optical and radio astronomy, deconvolution methods are widely used to increase the spatial resolution. For that purpose a variety of algorithms has been developed in the past, for example Non Negative Least Squares, NNLS algorithm. In recent years, the algorithms have been applied to acoustic array measurements and some of the most promising algorithms are the fast spatial FFT based De-convolution Approach for Mapping Acoustic Sources version 2, DAMAS2 and the FFT-NNLS. From a practical point of view, there are only minor differences between the two approaches, except that FFT-NNLS is a little slower but often more precise than DAMAS2.

The steps of the algorithms can be illustrated as follows. For a given array design monopoles are placed at a grid of positions covering the mapping area on the source plane. For each monopole position, i, a Delay-And-Sum (DAS) beamforming measurement is simulated and the pressure power distribution on the source plane is calculated. Thus the $\mathbf{PSF_i}$, which only depends on the test geometry, is obtained for each source location, i. See Figs. 2 and 3 for two examples.

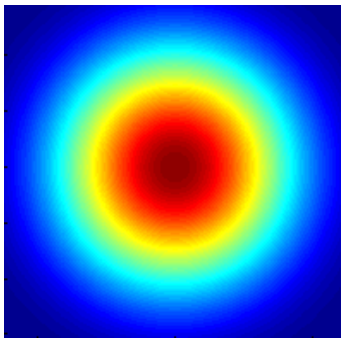

Fig. 2 – Point-Spread Function for an on-axis monopole at the focus plane

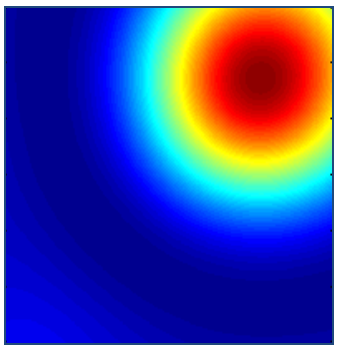

Fig. 3 – Point-Spread Function for a slightly off-axis monopole at the focus plane

For the actual array measurement an incoherent point source model is used and a solution is found in a least squares sense for non-negative monopole power strengths, i.e. $A_i \geq 0$, see Fig. 4.

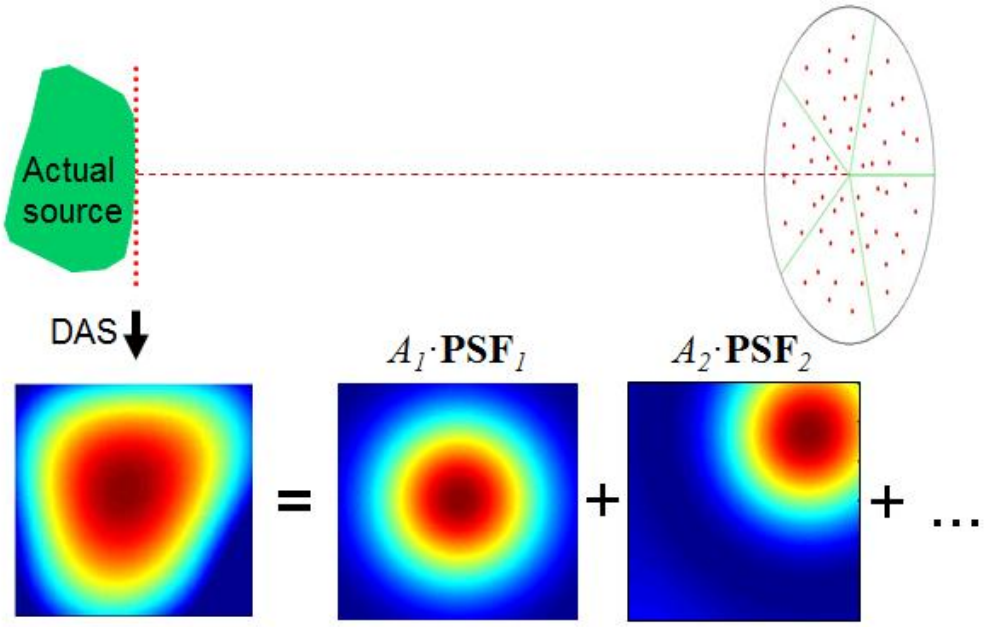

Fig. 4 – Incoherent source model is found in a least squares sense

The output from DAS is smeared by the individual $\mathbf{PSF_i}$. As an approximation, a position independent point-spread function (shift invariant across the mapping area) is assumed, so the one at the centre of the mapping area $\mathbf{PSF_0}$ is used in Eq. (5). Here, $\mathbf{A} = \{A_i\}$ is a matrix containing all the source strengths, and the symbol $\otimes$ represents convolution in x and y. Finally Eq. (5) is solved iteratively for **A** (deconvolution), which means that in practice the spatial resolution is improved compared to the original DAS by a factor 3-10, depending on the geometry of the array and test object. In practice approximately 50 to 100 iteration steps are enough.

$$\mathbf{DAS} \approx \mathbf{A} \otimes \mathbf{PSF_0} \qquad with \qquad \mathbf{A} = \{A_i\} \ and \ A_i \geq 0 \tag{5}$$

4. MEASUREMENTS ON RAIL VEHICLES

A measurement campaign was made to investigate the rolling noise of regional trains along the line of the north-south coastal route from Copenhagen to Helsingør in Denmark. The sound power of the

individual bogies was determined by means of Moving Source Beamforming measurements using a 2,5m diameter planar array (Fig.5). Each of the 9 arms, had 6 microphones spaced logarithmically from the centre of the array. All microphones were fitted with wind shields. To measure the speed of the train which was assumed to be constant for the duration of the passage through the measurement zone, trigger pulses were employed from two photocells, placed some 43m apart (Fig.6). A visible laser was used to align the triggers and measure the distances from the array to the rails. The trigger pulses were of different duration and thus the direction of travel of the trains could be determined and stored with the acoustical data.

Figure 5 – Logarithmic wheel array with 56 microphones and 9 arms used for measurements on trains

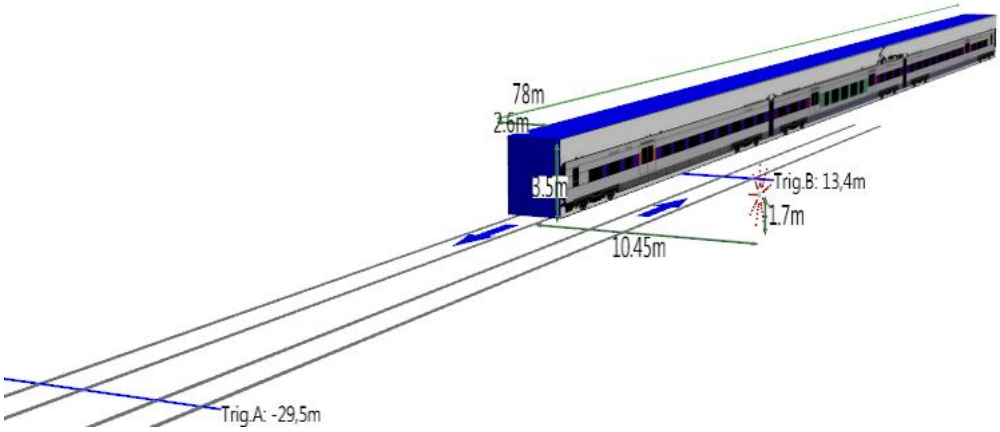

Figure 6 – An interactive site set-up with the positions of tracks, photocells and array to document the measurement campaign

The Maximum Side Lobe (MSL) of the 56 microphone beamforming array is given in Fig.7. It can be seen that the MSL is better than 7dB to beyond 12kHz. In situations where there is intrusive background noise, it is possible to fold or tilt such an array into the form of shallow cone which enables the noise incident from the rear to be reduced mathematically. However this configuration also increases the sidelobes of the array and thus reduces the MSL. For moving source beamforming, each measurement point on the train is tracked and the corresponding acoustic level averaged from the time the point enters into the opening angle of the array to the time it leaves. Thus the Doppler effect is automatically taken into account [6]. The chosen opening angle of the array is a compromise between

the requirement for high spatial resolution in the sound maps and a sufficiently long averaging time to reduce random fluctuations in the noise levels. It should also be noted that the resolution of the array decreases as the off-axis angle increases. The faster the train passes through the opening angle, the shorter the time available for averaging. For the trains in this measurement campaign, with speeds of around 120km/hr, the averaging time was about 0,4 sec.

After the installation of the array and the two photocells, which took less than an hour, moving source beamforming recordings were made for all the trains which passed by in the following 2 hours. All recordings were stored in a database with details of the trains which were composed of either 3 or 6 carriages. The speeds varied from 114 to 125km/hr. Permission to perform the measurements was obtained in advance from the railway authorities but no special safety regulations or security personnel were required as all measurement activities took place outside the boundary of the railway property.

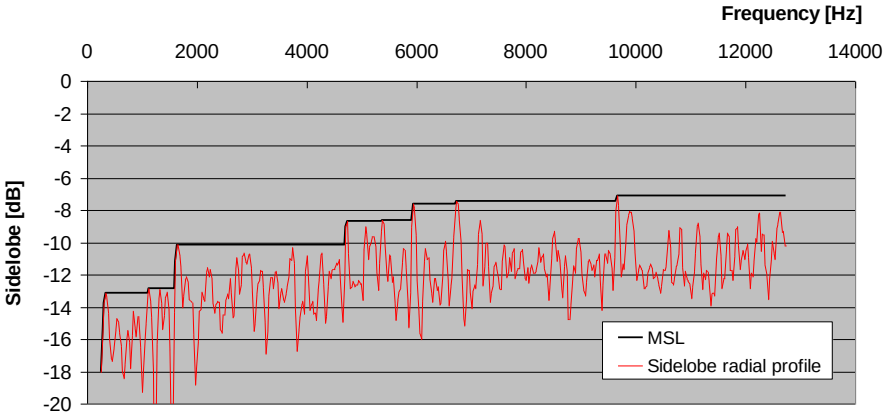

Figure 7 –Maximum Side Lobe suppression as a function of frequency for logarithmic wheel, foldable array with 56 microphones and 9 arms; fully unfolded, 2.5m diameter

On the same stretch of track, measurements were made as the trains passed through a local station without stopping. These measurements are not reported in this paper but in [7]. A 3,0m diameter, half wheel array, with 7 arms was used; each arm being equipped with 6 microphones (Fig.8). The hard level platform acted to a good approximation, as a reflecting mirror ground. The MSL of this 42ch array is better than 8dB up to 8kHz. With this measurement configuration, much of the rolling noise is shielded by the platform, so the noise from the pantographs could be more easily studied [7].

Figure 8– Half wheel array with 42 microphones and 7 arms used for measurements on through trains at a station. The reflectors for the photocell triggers can be seen on the opposite platform mounted on white boards (indicated by red arrows). The entire system was powered by a battery.

5. CALCULATIONS AND RESULTS

An inspection by eye and ear, of the recordings of the train pass-by data in the time domain, can often reveal the part of the signal of interest for further investigation (Fig.9). In Fig.9, the passage of

the bogies is clearly seen in the traces and can be clearly heard in the recordings. The bottom trace shows one bogie to be distinctly noisier than the rest. Apart from the basic tools of FFT and CPB and the usual forms of representation such as pressure contribution at the array, sound intensity on the surface of the train, sound power contribution from various parts of the train etc, the present system has a number of advanced parameters to reduce the effects of turbulence, excessive side lobes in the array and the coherence length in order to improve the noise source identification.

Figure 9 –Pressure signals as a function of time. Top: 3 carriage train, speed 121,6km/hr. Middle: 6 carriage train , speed 124,9km/hr. Bottom: 6 carriage train, speed 124,4km/hr. The bottom trace shows one bogie to be distinctly noisier than the rest (indicated by parentheses)

The diagonal removal technique [8] can be applied to suppress the contributions to the averaged spectra from the wind noise in the individual microphones and thus can yield clearer noise maps (Fig.10). Turbulence in the air will introduce a reduction of coherence over the extent of the array, and the coherence length will decrease as the frequency increases. This can be dealt with by applying a shading filter (area weighting) to the microphone signals so that only the central part of the array is used at high frequencies. The radius of the shading function is inversely proportional to the frequency which means that the microphone spacing must be denser at the central part of the array. Furthermore, the resolution of the array is inversely proportional to the array radius, but since the density of microphones is greater near the centre, the effective array size is smaller. For a given array this would affect the low to medium frequencies, where the entire array is used. To compensate for this loss in resolution, an additional weighting factor is applied to ensure a constant effective weighting per unit area over the active part of the array. Use of the array shading filter is particularly relevant with large arrays as the area associated with a particular microphone increases as the square of the distance of the microphone from the centre of the array.

The spatial resolution of the DAS maps can be further improved by applying deconvolution; in this case the NNLS algorithm is used. The output of the deconvolution is basically the strength of the monopoles allocated in frequency bands and distributed spatially.

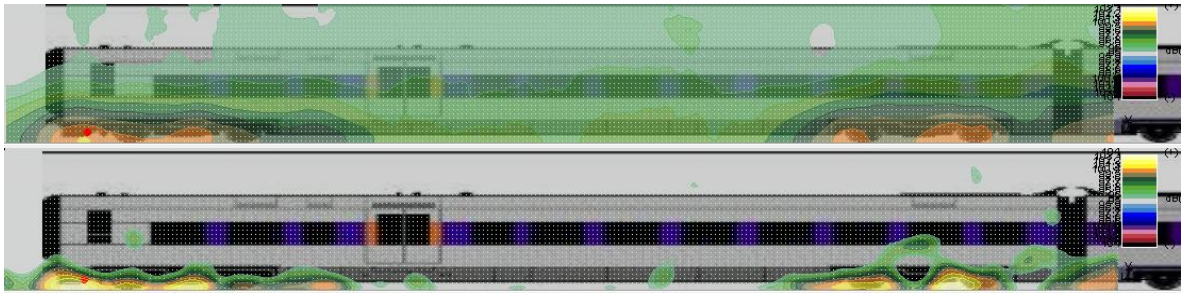

Figure 10 –Train moving at 114 km/hr to the left. Sound intensity contours with same scale, mapped on the surface of the train, frequency range 160Hz to 6368Hz. Top: DAS, no diagonal removal. Bottom: NNLS deconvolution, with diagonal removal

On the sound intensity contour maps of the six trains in the measurement campaign, the sound power from around the various bogies was determined within pre-defined areas (Fig.11). The same areas could be used on similar trains which improved the efficiency of the post-processing. An overview of all the sound power values is shown in Table 1. For train 11:56, the bogie 8 & 9 had a prominent sound power value. This bogie set was therefore chosen for more detailed mapping using the NNLS deconvolution algorithm, with the application of diagonal removal, and an array shading filter (Fig.12). The sound powers of the individual wheel sets were then determined and the quantified (Table 2). Bogie 8, wheel set 2 with a sound power of 109,7dB(A) was the main contributor to the noise.

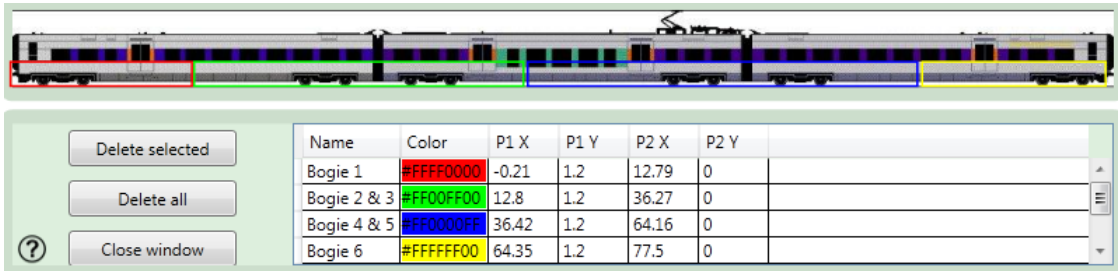

Figure 11 – Pre-defined areas over the various bogies for the 3 carriage trains under test

Table 1 –Sound power values for the individual bogies on the 6 trains.

				Sound power of bogies dB(A)						
Time	Nr. of carrriages	Direction of travel	Speed km/hr	Bogie 1	Bogie 2 & 3	Bogie 4 & 5	Bogie 6			
11:50	3	Left	122,6	107,9	111,1	111,4	107,3			
12:03	3	Right	121,6	97,6	102,9	102,2	97,3			
12:10	3	Left	114,4	107,4	110,0	111,0	105,9			
				Bogie 1	Bogie 2 & 3	Bogie 4 & 5	Bogie 6 & 7	Bogie 8 & 9	Bogie 10 & 11	Bogie 12
11:56	6	Right	124,4	104,6	109,9	110,0	110,4	112,7	110,0	106,3
12:01	6	Left	123,5	106,6	109,8	109,2	111,3	109,5	108,8	107,0
12:11	6	Right	124,9	104,3	109,2	109,7	109,2	109,1	108,7	106,4

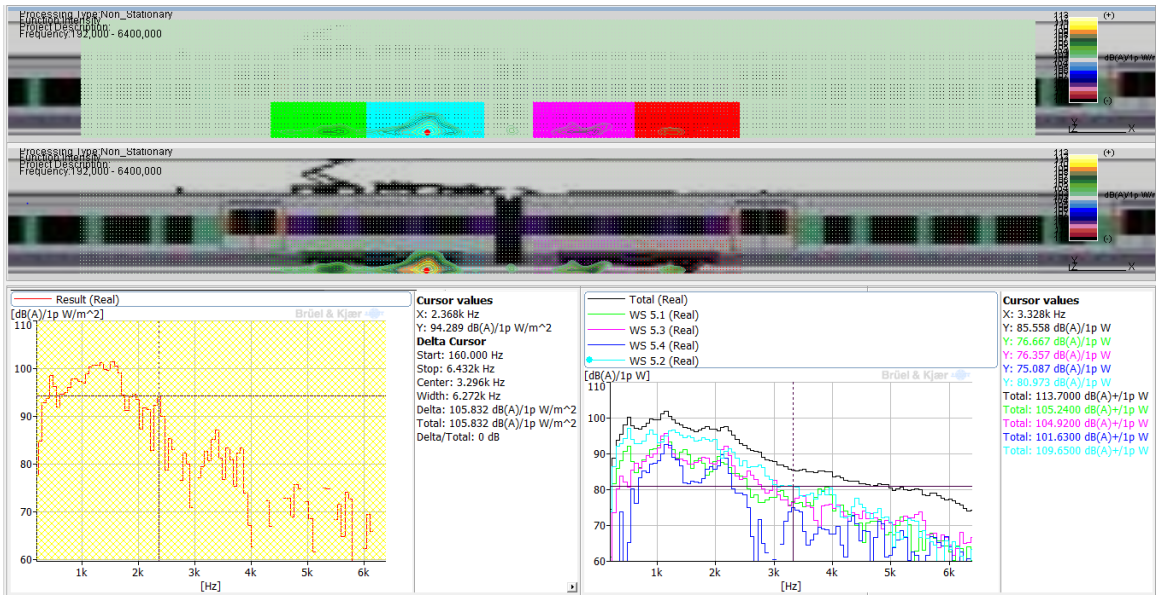

Figure 12 –. Upper plot shows the areas over bogie 8 & 9 of train 11:56 over which the sound power levels were calculated. Greyish green: total area for calculation. Lime green and light blue: wheel sets 1 & 2 of bogie 8. Pink and red: wheel sets 1 & 2 of bogie 9. Lower plot shows sound intensity contour map obtained using the NNLS deconvolution algorithm with "outdoor shading" filter. Graph on the left: sound intensity spectrum at the point marked with the red dot on bogie 8 wheel set 2. Graph on the right: sound power spectra over the four wheels sets.

Table 2 –. Sound power values dB(A) for the individual wheel sets of bogies 8 & 9

Time	Nr. of carrriages	Direction of travel	Speed km/hr	Bogie 8 WS 1	Bogie 8 WS 2	Bogie 9 WS 1	Bogie 9 WS 2
11:56	6	Right	124,4	105,2	109,7	104,9	101,6

6. SUMMARY AND CONCLUSIONS

This paper describes a practical microphone array system designed for noise source identification measurements on rail vehicles. The theory of beamforming methods is given together with a description of the deconvolution methods for increased spatial resolution. Various types of acoustical arrays suitable for rail vehicle measurements are discussed along with examples of use. For an investigation of the noise emission of trains along a particular section of track, the main sources of rolling noise were efficiently located by means of sound intensity maps and quantified in terms of sound power using moving source beamforming and deconvolution techniques. The entire measurement campaign was completed within 3 hours.

REFERENCES

[1] J. Hald and J.J. Christensen, "A novel beamformer design for noise source location from intermediate measurement distances", Proceedings of ASA/IFA/MIA (2002)

[2] J.J. Christensen and J. Hald, "Beamforming", Brüel & Kjær Technical Review no. 1, pp. 1‑48. (2004) http://www.bksv.com/Library/Technical%20Reviews.aspx?year=2004-2000&st=2004-2000

[3] J. Hald, "Combined NAH and Beamforming using the same Array - SONAH", Brüel & Kjær Technical Review no. 1, pp. 11‑50. (2005) http://www.bksv.com/Library/Technical%20Reviews.aspx?year=2012-2005&st=2012-2005

[4] Klaus Ehrenfried and Lars Koop, "A Comparison of Iterative Deconvolution algorithms for the Mapping of Acoustic Sources", American Institute of Aeronautics and Astronautics, AIAA Journal, Volume: 45, Issue: 7, pp. 1584-1595 (2007)

[5] Bernard Ginn and Jørgen Hald "Aerodynamic noise source identification in wind tunnels using acoustical array techniques" 8th MIRA International Vehicle Aerodynamics Conference - 'Low Carbon

Vehicles' (2010)
[6] J. Hald, Y.Ishii, T.Ishii, H.Oinuma, K.Nagai, Y.Yokokawa and K.Yamamoto, ”High-resolution Fly-over Beamforming Using a Small Practical Array”, Proceedings of AIAA (2012)
[7] Jesper Gomes, Jørgen Hald and Bernard Ginn, “Localising noise sources on a rail vehicle during pass-by”, IWRN13, International Workshop on Railway Noise (2013)
[8] Sijtsma, P. and Stoker, R., “Determination of Absolute Contributions of Aircraft Noise Components Using Fly-over Array Measurements,” AIAA Paper 2004-2958.